Chapter 9
A New Statistical-Empirical Hybrid Based Model to Estimate Seasonal Sea-Level Variation in the Gulf of Paria from River Discharge

Carol Subrath-Ali

Abstract The study presents new insight into the quantitative role of the world's third largest discharging river, the Orinoco of South America as modulating coastal water levels in the vicinity of its outflow. The case study is in a semi-enclosed sea, the Gulf of Paria, located in the southern extreme of the Caribbean Sea. The discharge – coastal water level relationship has been investigated and the water levels exhibit a high correlation ($R^2 = 0.92$) to the trends in actual discharge. The relationship is non-linear and there is a lower threshold value across the months of the year below which the water levels are characterised by large variability around a mean linear trend showing independence of the Orinoco's discharge. There is also an upper threshold value where the maximum amplitude of variation is 21.4 cm. The study utilises a vertically integrated 2D numerical modelling suite to execute a series of experiments to ascertain the variation of the coastal water levels from the variation in the river discharge. The other drivers are wind, salinity, oceanic currents and tidal forcing. The results are finally utilised to develop a third order model function to estimate the average monthly river-driven water level in the Gulf of Paria dependent only on the parameter of river discharge.

List of Symbols

C_D	Drag coefficient
d	Still water depth (m)
D	Eddy diffusion coefficient
f	Coriolis parameter (s^{-1})
F_T,F_s,F_c	Horizontal diffusion terms
g	Acceleration due to gravity (m/s^2)

C. Subrath-Ali (✉)
Department of Civil and Environmental Engineering, Faculty of Engineering, The University of the West Indies, St. Augustine Campus, St. Augustine, Trindad and Tobago
e-mail: subrath_ali@yahoo.com; carol.subrath.ali@gmail.com

C.W. Finkl and C. Makowski (eds.), *Remote Sensing and Modeling: Advances in Coastal and Marine Resources*, Coastal Research Library 9,
DOI 10.1007/978-3-319-06326-3_9,

h	Total water depth (m)
H	Height of Planetary Boundary Layer (m)
$\widehat{H}$	Source term due to heat exchange with atmosphere
p	Pressure (pa)
R	River discharge
s	Salinity (psu)
S	Magnitude of source discharge (m^3/s)
t	Time (s)
T	Temperature (°C)
x,y,z	Cartesian coordinates
u,v,w	Flow velocity components
η	Surface elevation (m)
ρ	Density of water (kg/m^3)
U	Wind speed
WL	Water level

Subscripts

a	Atmospheric component
h	Horizontal component
o	Initial condition (reference value)
s	Source parameter
v	Vertical component

9.1 Introduction

The purpose of this chapter is to present a newly derived formulation to estimate the contribution to coastal water levels in a semi-enclosed sea, from driving effects of seasonal, river driven, freshwater flux into the coastal environment.

It is well known that higher coastal water levels (WLs) from coastal setup can exacerbate shoreline erosion, reduce bottom friction with the inland movement of the water line and in so doing, amplify the tidal range and serve to alter the coastal morpho-dynamics. Coastal setup, generally defined as the temporary elevation of coastal WLs may be observed as the slope on the water surface or the rise in the mean sea level towards the shore from the combined effects of wave, wind and barometric pressure (Allen 1997; Loveless et al. 1998). These short term sea level variations of coastal WLs have been shown to have several orders of magnitude greater than the trend (Kolker and Hameed 2007).

Previous researchers have examined the effects of these varying coastal processes mainly along the individual veins of wave set-up [temporary sea level elevations from breaking waves] (Dean and Walton 2010; Stockdon et al. 2006; Gourlay 1992), wind set-up [temporary sea level elevations from transfer of momentum by wind stress effects] and a pressure effect from a decrease in atmospheric loading [the inverse barometer effect].

While the major impacts from these effects may be more noticeable during an extreme event, the climatic characteristics of the individual variables however usually introduce an element of seasonality. One such other seasonal but infrequently considered driver is the freshwater flux into the coastal environment from river discharge. Although the term "river setup" is not defined in the literature, the concept has been examined although quantitative studies are not quite common. It is however acknowledged that river runoff can induce large-amplitude seasonal variation of the sea level in regions located near river outflows (Tsimplis and Woodworth 1994; Meade and Emery 1971). These elevated WLs with varying residence times can impact salinity stratification, effluent dispersion rates and engineering activities.

It is acknowledged that each coastal site will host varied coastal processes due to the native environment (for example: bathymetry, topography and shoreline configuration); as such, riverine discharge influences are not expected to be globally homogeneous. This paper then, examines a case study site where the coastline is affected by the world's third largest discharging river – the Orinoco, which discharges from north-eastern Venezuela of the South-American continent, directly in part into a semi-enclosed bay – the Gulf of Paria (GoP). The formulation is based on numerical, experimental methods utilising a vertically integrated 2D hydrodynamic model – the MIKE 21 Flow Model HD FM model, as well as incorporating statistical methods by the use of k-means cluster and regression analyses.

9.1.1 Global Freshwater Influence

Freshwater flow has been assessed for its contribution to coastal WLs in various parts of the world. Some illustrative examples of river discharge contribution to seasonal sea level change include the Chanjiang Estuary in China which has an annual sea level variation from 40 to 70 cm. The most significant factor in causing this variation is the river runoff (Baocan et al. 1992). In the Bay of Bengal, river runoff produces a WL variation of 100 cm within a year (Pattullo 1966) and along the eastern United States, variations in annual runoff inflow account for 7–21 % of the total sea level variation from 1 year to the next (Meade and Emery 1971). Varying levels of the Black Sea bounded by Europe, Anatolia and the Caucasus, are closely related to river discharge from the Danube. In Varna Bay in the Black Sea, the maximum amplitude of variation is 16.1 cm (Trifonova and Demireva 2003). River runoff has also been described as a considerable factor causing sea level changes both in an estuary as well as the adjacent coast. The largest reported variation at 100 cm/year occurs in the Bay of Bengal (Pattullo 1966).

Since steric effects are usually considered as the combination of salinity and temperature effects, the changes from these may manifest themselves from either internal oceanic changes such as upwelling, or the entrainment of freshwater into the more saline sea water. Some of the difficulty of estimating the forcing from river discharge lies in the separation of these processes. Nonetheless, as shown above, there have been studies which have examined the effect of riverine, freshwater flux

on coastal WLs. The effect however, has been particularly dominant in estuaries with large salinity slopes and the variation has been described as being dominant on a suggested time scale of a few days (Bjork et al. 2000).

While volumetric freshwater flow has been discussed as one of the factors affecting sea level, the variation has also been ascribed to being heavily dependent on the density of sea water (Nomitsu and Okamoto 1927). This density variation has generally been defined in terms of the seasonal fluctuations in the specific volume of sea water (Lisitzin 1974) and can be expected to exhibit significant changes in regions where there is an influx of freshwater such as in the vicinity of river outflow.

With regard to the relationship between seasonal river discharge and WL variations, there are comparatively few studies that have informed us of quantitative relationships to enable the use of the volumetric discharge for these non-tidal elevation estimates. While earlier researchers (Nomitsu and Okamoto 1927; Galerkin 1960; Lisitzin and Pattullo 1961; Pattullo 1966; Meade and Emery 1971; Svensson and Jones 2004) have noted the river contributions, quantification of the discharge – sea level variation relationship has been less forthcoming; perhaps because of the vast number of signals that contribute to the overall variation of the coastal WL making the task far from straightforward in most cases.

In addressing the relationship between river discharge variations and coastal WL elevations, it is useful to quantify the relationship so that an assessment of the elevation can be made in a predictive mode. A relationship of this kind is not expected to be universally applicable to estimate sea level variation from freshwater flux due to the variations in site-specific characteristics. The development of the relationship can however, provide a useful tool for a given region and will further provide an economic means to estimate the seasonal, freshwater contribution to the coastal WL in the relevant coastal environment. Applicable areas are coastal engineering, port and harbour development and the provision of baseline information to coastal flood defence strategies.

The chapter next presents an overview of the study area and the data and methodology employed to execute the study. The results and discussion then follow and the chapter then concludes on the results of the findings.

9.1.2 Study Area

The site of interest is located in the extreme south-east of the Caribbean Sea, off the South American continent (Fig. 9.1), situated between extreme north-eastern Venezuela and the southernmost Caribbean island – Trinidad. The semi-enclosed water-body, the GoP, covers an area of roughly 7,600 km^2 and at its widest, measures approximately 150 km, at its narrowest about 14 km. It is generally shallow with average depths of about 20 m (van Andel and Postma 1954; Gade 1961).

The largest river which discharges directly into the GoP from Trinidad is the Caroni with an average flow rate of 12 m^3/s (Environmental Management Authority 1998). The Orinoco River originates in Venezuela and discharges waters amassed

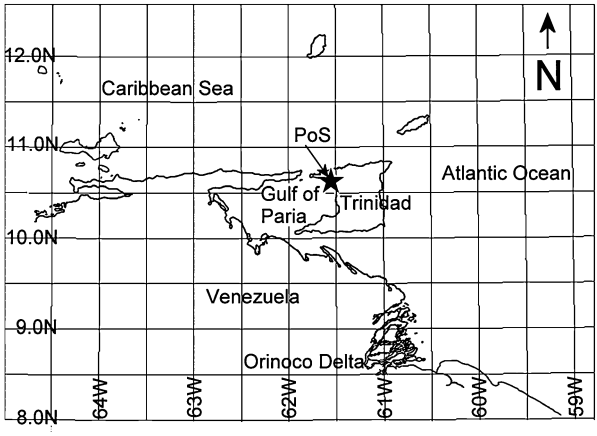

Fig. 9.1 The location of the Gulf of Paria in the southern Caribbean

from an approximate 31 major and 2,000 minor tributaries into the western tropical Atlantic Ocean largely through the Orinoco Delta (Odriozola et al. 2007). It is the third largest river volume discharge in the world with an average of about 3.6×10^4 $m^3\ s^{-1}$ (Meade et al. 1983; Müller-Karger et al. 1989) to the Atlantic Ocean. Since the Orinoco directly empties in part into the GoP, there are a variety of coastal and dynamic influences from its discharge. The effects have been examined with respect to rainfall over the Orinoco watershed region (Schot et al. 2001), seasonal control of salinity in the eastern Caribbean (Froelich et al. 1978), river water plume dispersal by examining ocean colour (Hu et al. 2004) and sediment input into the eastern Caribbean (Bowles and Fleischer 1985). There have been no comprehensive studies however, on the quantitative effect of the freshwater flux from the Orinoco and the forcing of the WL in this coastal environment. What makes this study of particular interest is the fact that the largest distributary which accounts for a near 85 % of the discharge, does not flow directly into the GoP, but discharges at some 114 km away.

The climate of this tropical area is strongly reflected as being bi-seasonal. The two seasons differ primarily by precipitation with the migratory Inter-Tropical Convergence Zone (ITCZ) playing a key role in the precipitation patterns. The dry season (January to May) is characterised by relatively lower precipitation and the wet season (June to December) is characterised by heavier precipitation. The latter hosts the Atlantic hurricane season (June to November). The dominant wind regime is primarily governed by the north easterly trade winds.

While it is well noted that common sea level forcing mechanisms include drivers such as tides, winds, offshore waves and river discharge as well as their combination (Brown and Kraus 2007); there are however, other additional parameters that may or more aptly, should, be considered such as the bathymetry and topographic configuration, But as Svensson and Jones (2004) point out, to address the site specific nature of river flow characteristics a dense network of gauges would be required.

To adequately address the site specific effects of a given river outflow using such a dense network is however, not easily accomplished. For example, in the study of

the oceans, a conservative, economic estimate for tidal observations at a one degree resolution to study the oceans at a needed 45,360 observation sites would cost nearly half a billion dollars per year, with an enormous time budget and at least a 45 year timeline for the project (Parker 1991). To overcome such problems, the use of numerical models has, within recent time, become increasingly popular to investigate the behavior and effects of coastal processes.

9.1.3 Numerical Modelling

The 2D hydrodynamic, propriety "MIKE 21 Flow Model HD Flexible Mesh" model of the Danish Hydraulic Institute is employed to execute a series of numerical experiments to assess the coastal WL response in the GoP to the Orinoco's discharge. This model is designed to simulate flows and WLs not only in bays and estuaries but in other coastal areas. The model is capable of constant and varying complex flow conditions (in terms of depth, average velocity and flow direction) which may be laterally unsteady across the width of the flow and resolves flows with variable directions (unlike 1-D models). Additionally, the model's suitability for the study area is based on the physical characteristics of the site; such as its shallow nature (20 m average depths). The 2D model also reduces the computational expenditure that would otherwise be incurred with the use of a 3D model.

The basic, governing equations are all based on the 3D Navier-Stokes equation and the main equations which are integrated over depth are:

$$\frac{\partial u}{\partial x}+\frac{\partial v}{\partial y}+\frac{\partial w}{\partial z}=S \tag{9.1}$$

where (9.1) is an expression of the local continuity equation.

The x component of the horizontal momentum equation is given by:

$$\begin{aligned}\frac{\partial u}{\partial t}+\frac{\partial u^2}{\partial x}+\frac{\partial vu}{\partial y}+\frac{\partial wu}{\partial z}&=fv-g\frac{\partial \eta}{\partial x}-\frac{1}{\rho_0}\frac{\partial p_a}{\partial x}-\frac{g}{\rho_0}\int_z^{\eta}\frac{\partial \rho}{\partial x}dz+F_u\\&+\frac{\partial}{\partial z}\left(v_t\frac{\partial u}{\partial z}\right)+u_sS\end{aligned} \tag{9.2}$$

the y component of the horizontal momentum equation:

$$\begin{aligned}\frac{\partial v}{\partial t}+\frac{\partial v^2}{\partial y}+\frac{\partial vu}{\partial x}+\frac{\partial wv}{\partial z}&=-fu-g\frac{\partial \eta}{\partial y}-\frac{1}{\rho_0}\frac{\partial p_a}{\partial y}-\frac{g}{\rho_0}\int_z^{\eta}\frac{\partial \rho}{\partial y}dz+F_v\\&+\frac{\partial}{\partial z}\left(v_t\frac{\partial v}{\partial z}\right)+v_sS\end{aligned} \tag{9.3}$$

the general transport-diffusion equation for temperature and salinity:

$$\frac{\partial T}{\partial t}+\frac{\partial uT}{\partial x}+\frac{\partial vT}{\partial y}+\frac{\partial wT}{\partial z}+\frac{\partial wT}{\partial z}=F_t+\frac{\partial}{\partial z}\left(D_v\frac{\partial T}{\partial z}\right)+\widehat{H}+T_sS \tag{9.4}$$

$$\frac{\partial s}{\partial t}+\frac{\partial us}{\partial x}+\frac{\partial vs}{\partial y}+\frac{\partial ws}{\partial z}=F_s+\frac{\partial}{\partial z}\left(D_v\frac{\partial s}{\partial z}\right)+s_sS \tag{9.5}$$

The definition of the horizontal diffusion terms is as follows:

$$(F_T,F_s)=\left[\frac{\partial}{\partial x}\left(D_h\frac{\partial}{dx}\right)+\frac{\partial}{\partial y}\left(D_h\frac{\partial}{dy}\right)\right](T,s) \tag{9.6}$$

The reader can refer to DHI's scientific documentation (Danish Hydraulic Institute 2011) for the full description of the governing equations.

9.2 Data and Method

This section is discussed in two parts. The first part presents the data (as referenced to the mesh in the second part). The second part of the method looks at the generation of the mesh, data treatments and execution procedures of numerical model experiments. It uses the results to develop the statistical model to estimate riverine driven WLs from a given discharge.

9.2.1 Data

Since no observed tidal data were available along the open boundaries (south, east and north) (Fig. 9.2) on the model domain, tidal boundaries were created using the tidal prediction capacity of the inbuilt MIKE 21 Tidal Toolbox by using the defined boundaries of the model. The tidal values along all open boundaries were created in this manner and the forcing was verified using measured data inside of the domain at Port of Spain (PoS, Fig. 9.1). Measured, hourly tidal values at PoS for 1987 are available.

The Guiana current data were input as a monthly 1×1 degree spatial u and v velocity component grid derived by an Objective Analysis (OA) scalar subroutine (Mariano and Brown 1992) represented by the Mariano Global Surface Velocity Analysis (MGSVA) (Mariano et al. 1995). This resolution is justified on the basis on the strength and persistence of the Guiana current (Boisvert 1967) with the majority (80–85 %) of scalar currents found in the range (0.41–1.2) m/s (Febres-Ortega and Herrera 1976) and another estimate in the (0.1–2.2) m/s range found by Boisvert (1967).

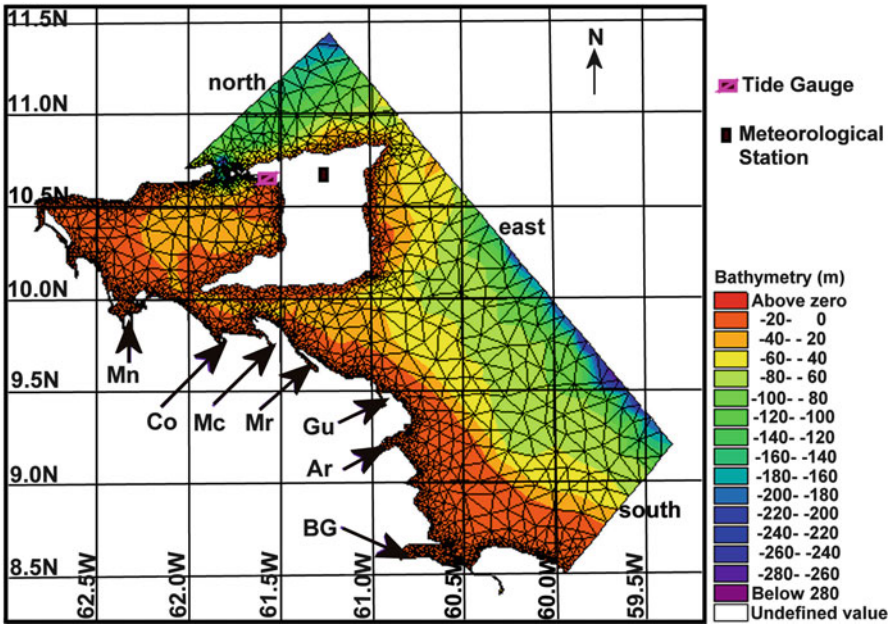

Fig. 9.2 Mesh created for the model domain. The seven major distributaries are designated: BG-Boca Grande; Ar-Araguao; Gu-Guiniquina; Mr-Mariusa; Mc-Macareo; Co-Cocuina; Mn-Manamo

Depth averaged oceanic salinity data were extracted from the World Ocean Atlas (WOA09) (Antonov et al. 2010) database for the monthly variations utilizing data along the boundary and where not available, the nearest gridded value from an objectively analyzed (1×1 degree grid) climatological salinity field.

Hourly observed wind data were sourced from the island of Trinidad (TTMS 2010) and were taken to be representative of the wind field and allowed to vary in time but taken as constant in the domain but with a varying Coriolis force to allow veering of the vectoral wind. This domain representation was based on the persistent nature of the north-easterly trade winds (meteorological convention). The wind drag coefficient of 0.001255 was applied (over water wind speeds of average 7 m/s).

The bathymetry used, is a combination of data extracted from MIKE C-Map for the wider oceanic region of the model domain and locally surveyed depths in the GoP by a local consultant company. MIKE C-Map is a DHI software tool for extracting depth data and predicted tidal elevation from the world-wide Electronic Chart Database CM-93 Edition 3.0 from C-Map Norway (Danish Hydraulic Institute 2011).

The river discharge data were sourced from a hydrological database: *The Global Runoff Data Centre, 56068, Koblentz, Germany*, as monthly data from gauging stations at Musinacio (7.69 N 64.76 W) for the period (1970–1992) and daily data

from Puente Angostura (8.15 N, 63.6 W) for (1973–1989). Data for each of the distributaries are not available and an appropriate procedure, as discussed in the data treatment method was used to distribute the waters according to the seven (as guided by literature) major outflows.

9.2.2 Mesh Generation and Boundary Conditions

An unstructured, triangular mesh (Fig. 9.2) was generated using digital bathymetric, shoreline and water data with the vertical datum as mean sea level and the map projection system UTM20. The defined area was selected such that the major outflow channel of the Orinoco Delta (the Boca Grande) towards the southern end is accommodated within the model domain. The outflow from the GoP into the Caribbean Sea at the northern end was similarly accommodated.

The mesh boundary conditions were defined so that there are three open boundaries (south, east and north) and one land boundary (the continental coastline, bounding Venezuela). The varying triangular elements are such that on the open boundaries the resolution is at 10 km on the flexible mesh, to a smaller grid spacing of 250 m inside of the GoP. This spacing was chosen in consideration of the large scale forcing on the boundaries as well as in keeping the number of elements to a minimum as possible to ensure reasonable run-time on the available computing system (a finer mesh of a 10 m grid size increased the computational time from 5 to 32 h per run). The entire mesh domain area is greater than, but estimated near 48,000 km^2.

The south boundary defines the major inflow boundary into the model domain with regard to forcing from the oceanic currents. This boundary is aligned at a quasi-perpendicular orientation to the closed boundary and the inflowing major dominant current – the large-scale Guiana current regime which exhibits a persistent flow from south-east to north-west throughout the year. The seaward extent of the south boundary is near the edge of the continental shelf at the 200 m isobath depth where it connects to the east boundary.

The east boundary is aligned along the major dominant flow of the Guiana currents (towards the northwest) and is approximately along the shelf break at the 200 m isobath.

The northern boundary is oriented in a similar fashion to the south boundary but is essentially an outflow boundary with regard to the main current flows and as such is quasi-perpendicular to the north-westward, heading Guiana current.

The seven major sources of freshwater discharge from the Orinoco Basin defined within the model domain, account for the distribution of the cumulative discharge from the many distributaries which enable the river water to reach the Atlantic. This distribution procedure is further discussed in the second part of the data treatment method.

9.2.3 Data Treatment Method

Ideally, the wind data along the boundaries are needed for wind forcing. As such, wind parameters over the sea were calculated according to an expression developed by (Hsu 1981) which uses wind speed (U), height of the planetary boundary layer (H) and wind drag coefficient according to Eq. 9.7:

$$\frac{U_{sea}}{U_{land}} = \left[\frac{H_{sea} \times C_{D\ land}}{H_{land} \times C_{D\ sea}}\right]^{1/2} \tag{9.7}$$

The subscripts "sea" and "land" denote the offshore and onshore states respectively. Values for the $\frac{U_{sea}}{U_{land}}$ ratio have been suggested as 1.7 (SethuRaman and Raynor 1980) and 1.6 $\pm$ standard deviation (Hsu 1981), it is also noted that the ratio varies with distance offshore with an average value given as 1.6 at a distance of 20 km offshore at a 10 m height. The correction by such a ratio did not however, address the condition of calm. The regression model developed by (Hsu 1985) was used and the corresponding wind directions were linearly interpolated.

$$U_{sea} = 1.62 + 1.17U_{land} \tag{9.8}$$

The use of such a constructed dataset produced erratic variations on the model results are the constructed winds were clearly not representative of the actual vectoral wind. The use of the meteorological data was reverted to, and is taken as the driving wind field throughout the domain but varying in time.

Since the distributary flow rates are not available except for a fractional estimate at the Boca Grande, an approximation of the hourly flows at Barrancas (Fig. 9.3), at the top of the delta, was utilised. A river flow, disaggregation method (Acharya and Ryu 2014) was employed to increase the resolution on the Musinacio time series (longer running dataset) using 3 month daily historical window on data at Puente Angostura. A correction of 11 % (Lewis and Saunders 1989) was added for the significant contribution from the Caroni River (Venezuela) and the other runoff and direct precipitation were considered negligible.

The streamflow estimates at Barrancas were distributed among the seven largest caños (Boca Grande, Araguao, Guiniquina, Mariusa, Macareo, Cocuina, Manamo) (Fig. 9.2) each according to their carrying capacity as a fraction of the total Barrancas flow rates.

Since the Boca Grande (the primary distributary) is known to account for about 85 % of the river flow, the major remaining secondary distributaries account for fractions of the remaining 14 % (-1 % for unaccounted for processes).

The discharge was distributed according to the cross sectional carrying capacity of each of the remaining six major channels (using the channel cross-sectional width near outflow and average bathymetric depth). Each channel's (Boca Guanipa, Cocuina, Macareao, Mariusa, Guanipa, Araguao) outflow capacity was estimated and assigned a fraction of the total of the six combined so that each carries a fraction

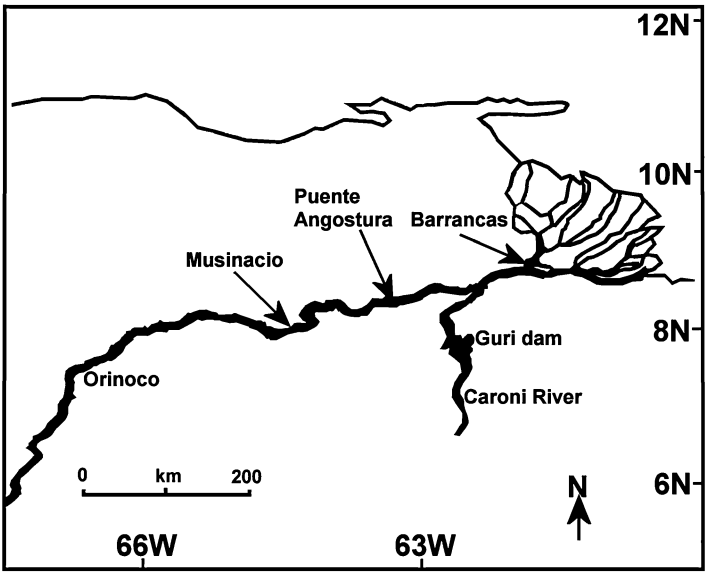

Fig. 9.3 The approximate locations of the gauging stations at Musinacio, Puente Angostura and Barrancas

of the remainder of the waters, not discharged through the Boca Grande, flowing out to the ocean. In this way, the bulk volume of water that is estimated at Barrancas is distributed such that it collectively reaches the Atlantic.

9.2.4 Model Execution Procedures

The hydrodynamic model is driven with data for the entire year of 1987. This particular year has been selected because of the availability and gap-free attributes of the all the required datasets of tides, winds, salinities and oceanic currents. The statistical model is developed with monthly river discharge data for a 23 year period (1970–1992). The open east and south boundaries are forced with changes in the parameters of tides, oceanic currents and salinity, except for the north boundary where currents are not specified. This allows the movement of water through the domain to flow out guided only by the inflow attributes. The closed, land boundary is set to a zero-normal flux velocity.

MIKE 21 offers two choices for time integration and space discretization in the solution of the shallow water equations. These are a lower order, fast algorithm and a higher order solution. At the expense of increased computational time, the higher order was chosen since the flow is convection-type and also to enables a higher level of accuracy. Stability in the transport equations was maintained by holding the critical CFL number to 0.8 (the recommended value is less than 1). To facilitate

turbulence in the water body from mixing, due to large velocity gradients as produced by the high flow rates from the Orinoco, the condition of turbulent velocity is accounted for by the Smagorinsky eddy viscosity formulation of a constant value of 0.28. A low bed resistance was applied with a Manning's coefficient of 40 at the higher range of recommended values (20–40 $m^{1/3}/s$) as the output of river-borne sediments consists of fine material, about 85–95 % suspended silt and clay (Warne et al. 2002).

The model's simulations are scenario analyses, executed for a full year (1987). Each month's WL in the GoP was simulated by gradations of 10 % (−50 to 50 %). Monthly initial water levels were also simulated by turning off all sources (that is a zero discharge). To establish a given month's flow, the model was given a soft start and allowed to initialize or enter a convergence phase by execution from the previous month. In this way any 1 month's simulation is the latter month's result from a 2 month run at a computational time of approximately 5 h for each execution.

9.2.5 Calibration and Validation

The river discharge data which were disaggregated using Acharya and Ryu's (2014) method allow compatibility on hourly estimates and enable hourly flow rates to facilitate WL estimates in the GoP that are as close as possible to the measured tide gauge values.

Model runs are done in parallel at the calibration stage using the hourly disaggregated flows as well as the monthly averaged values interpolated with a cubic, shape – preserving function. When the model outputs are compared to the observed tide gauge values, the use of the monthly river discharge data results a lower RMSE value than the use of the hourly disaggregated flow consistently across the majority of the months (Fig. 9.4) with the same RMSE for February and marginally higher values for April, September and December. Since the goal of parameter estimation for numerical modelling is to ultimately reduce the error between modelled and observed values, the monthly, interpolated values are utilised for the simulation routine.

The calibration exercise uses the spring/neap cycles for the months of low (March) and high (September) discharge. Measured tide gauge values are utilised inside of the model domain at the tide gauge location in the north GoP at Port of Spain.

The model's results are adjusted for phase lag (GMT/LST) and a WL adjustment at a 0.71 m (the vertical datum is 0.73 m below MSL). The model is validated for all the months of 1987.

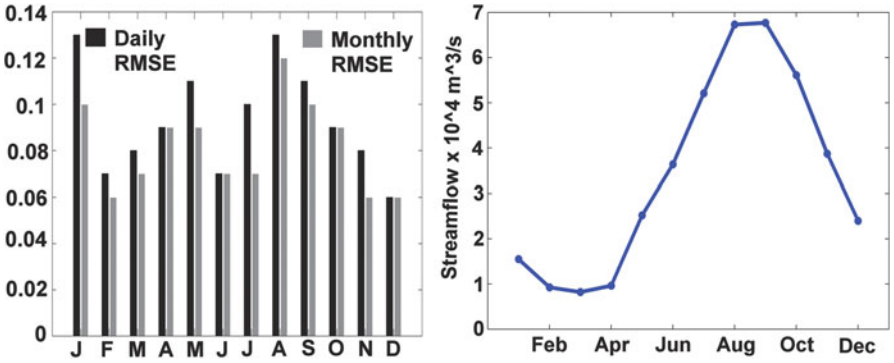

Fig. 9.4 Error variation in the use of the 1987 daily vs. monthly streamflows; the 1987 hydrograph is shown in the *right panel*

9.2.6 Development of the Statistical Model

Based on the output of the model runs, the WLs which reflect the monthly influence of the driving stream-flow are analysed by regression procedures to obtain a function for the discharge/WL relationship for that month for 1987.

The functions are then used to estimate the WLs across each month driven by discharge for the period (1970–1992) and the resulting WLs were phase lagged and used to develop a statistical relationship between both parameters. The result is a statistical model which can adequately estimate the riverine-driven variation of WL based on the discharge value only.

9.3 Results and Analysis

9.3.1 Validation of Modelled Water Levels

The validation data to assess the model's ability to adequately represent the real world hydrodynamic environment across all the months for 1987 are presented as scatterplots in Fig. 9.5 and the RMSE (root mean square errors) of the observed vs. the modelled WLs are shown.

The monthly WL averages, associated Pearson's correlation coefficient (R) coefficient of determination (R^2) and RMSE values between the modelled and the measured WLs for the composite scatterplots in Fig. 9.5 are shown in Table 9.1.

The largest measure of scatter as indicated by an R^2 value of 0.81 occurred during August with May and September also exhibiting high scatter with the R^2 values of 0.88 and 0.82 respectively. The largest measure of error occurred during August assessed by a RMSE of 0.12, with September and January also having

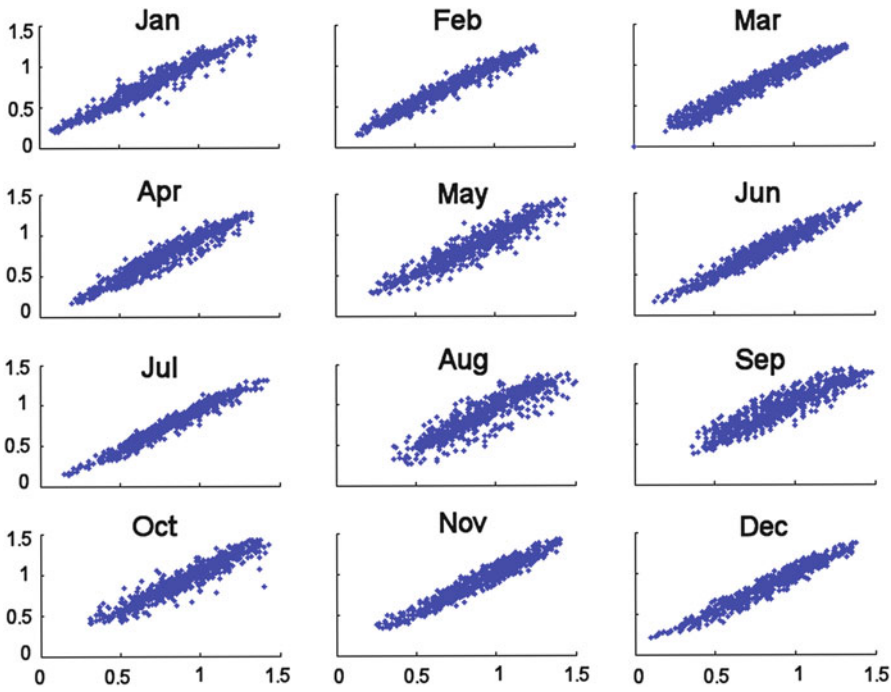

Fig. 9.5 Scatterplots of the observed vs. the modeled WLs for 1987

Table 9.1 Measured and modelled monthly mean water level statistics for scatterplot panel in Fig. 9.4

Month	Measured	Modelled	R	R^2	RMSE
Jan	0.72 ± 0.26	0.80 ± 0.26	0.97	0.94	0.10
Feb	0.71 ± 0.26	0.73 ± 0.25	0.98	0.96	0.06
Mar	0.73 ± 0.27	0.72 ± 0.26	0.97	0.94	0.07
Apr	0.79 ± 0.26	0.75 ± 0.26	0.96	0.92	0.09
May	0.87 ± 0.26	0.85 ± 0.25	0.94	0.88	0.09
Jun	0.81 ± 0.25	0.80 ± 0.25	0.97	0.94	0.07
Jul	0.84 ± 0.25	0.78 ± 0.25	0.98	0.96	0.07
Aug	0.92 ± 0.24	0.87 ± 0.25	0.90	0.81	0.12
Sep	0.91 ± 0.25	0.94 ± 0.24	0.91	0.82	0.11
Oct	0.90 ± 0.25	0.95 ± 0.24	0.95	0.90	0.09
Nov	0.89 ± 0.25	0.91 ± 0.25	0.97	0.94	0.06
Dec	0.83 ± 0.26	0.84 ± 0.25	0.97	0.94	0.06

RMSEs of 0.11 and 0.10 respectively. It is noted that August and September are months where maximal flows occur, with August being a near stationary point on the hydrograph (Fig. 9.4, panel B).

Based on the spread of the RMSE across the months, the model is assessed as adequately representing the hydrodynamic conditions within the GoP despite the lower R^2 and higher RMSEs across some months.

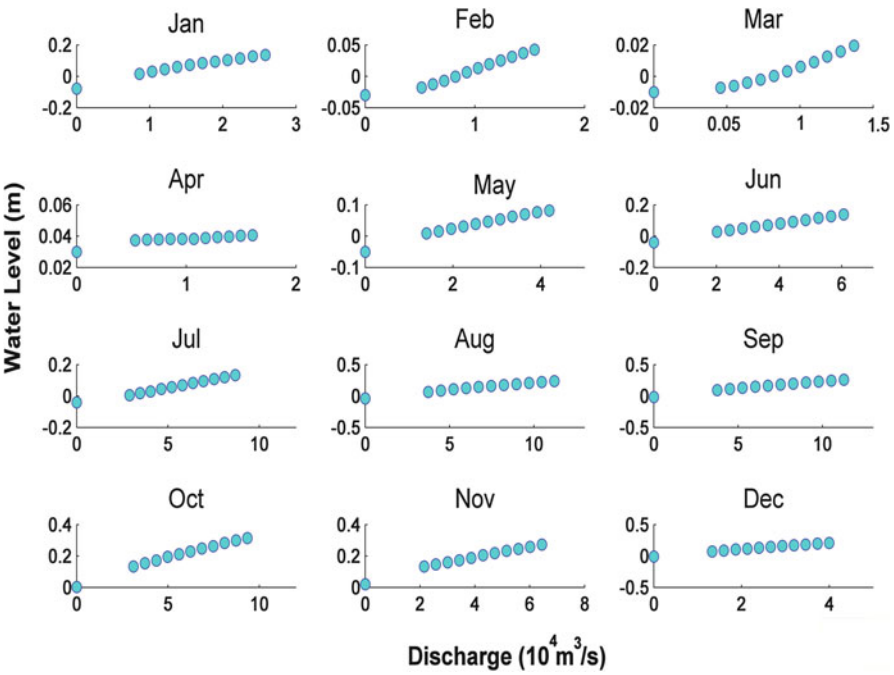

Fig. 9.6 Results of water level response to variation in river discharge

9.3.2 Statistical Water Level Estimates

The model setup, when used to execute the series of numerical experiments where the river discharge was varied at increments of 10 %, provides results (Fig. 9.6) of the numerical simulations thus enabling the monthly formulation of the river-driven, WL/discharge relationship. The results represent the changes in the WL for corresponding changes in the discharge.

Regression analysis by a method of least squares was utilised to formulate the relationship and the lowest order polynomial was selected according to the highest coefficient of determination that is, for any R^2 over 0.99 a quadratic fit was made. April was the only month that did not enable a fit over 0.99 for a second order polynomial ($R^2 = 0.94$) and a third order polynomial was employed. The May's scatter values produced a relationship that presented averaged WL values which were anomalously high. This result was deemed an outlier and the values were re-adjusted to conform to the trend of the monthly plots. The composite scatter for the WL/discharge relationship from the model simulations are shown in Fig. 9.6.

The resulting equations from each month, when applied to estimate the monthly WL variation over the 23 year period (1970–1992) for which the Orinoco's flow rates are available, produced a heterogeneous plot. This is demonstrated by the scatterplot, top left panel in Fig. 9.7 which shows the discharge vs. WL for each

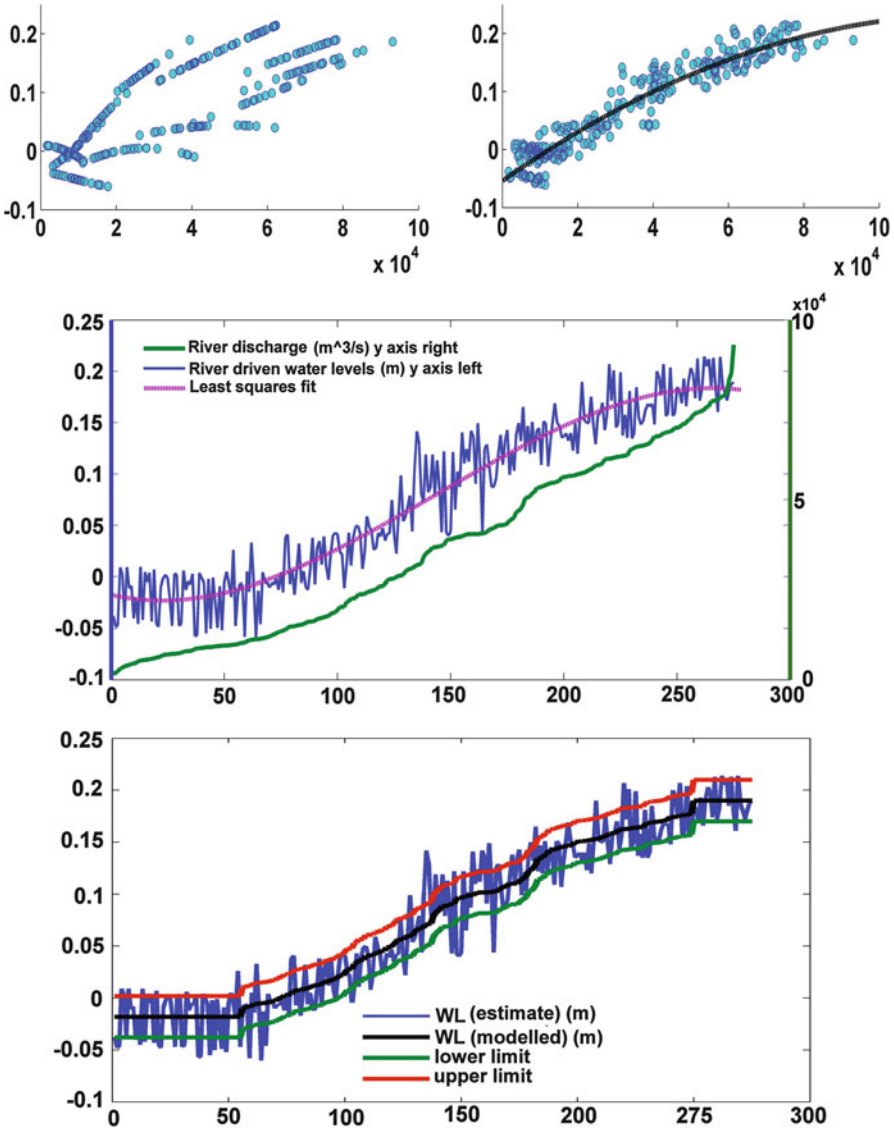

Fig. 9.7 Discharge/water level relationship (1970–1992). *Top panels* shows the relation between the river discharge ((m^3/s), x axis) and the WLs ((m), y axis) with cross correlated signals *top right*. *Middle panel* shows the river discharge and the corresponding phased WLs for ascending values of river discharge. *Bottom panel* shows upper and lower limits on WLs for the lower threshold, rising limb and upper threshold of the modelled function

month maintaining it's integrity with some overlap. When however, the WLs are phased by 1 month's lag as shown in the top right panel there is a clear relationship between the WLs and the previous month's discharge with a high regression coefficient (0.92).

All of the calculated WLs, when sorted according to the increases in the river discharge produced a third order polynomial fit ($R^2 = 0.90$) across the 23 years. The sorted WLs/river discharge data as shown in the bottom panel in Fig. 9.7 indicate that there is a lower threshold value below which the variations in the coastal WLs are independent of the river flow rates and there is also some upper threshold upper limit where the curve levels.

K-means clustering for three clusters suggested by the last regression fit provides the three separate cluster means of −0.01 cm, 0.05 cm and 0.16 cm although the silhouette plot indicates that the first two clusters are not well separated. By accounting for 98 % of the WLs below 0.01 m the threshold value for discharge is 10,000 ($+2.3 \times 10^3$) m^3/s, below which there is no significant trend. At the upper limit, the curve flattens out with the upper threshold at 70,000 ($+5.2 \times 10^3$) m^3/s.

Thus, 90 % of the WL values above the lower threshold can be then estimated by third order polynomial Eq. 9.9, with a standard deviation of ±0.08 m.

$$y = \left[\left(-4E(-16)R^3\right)\right] + \left[3E(-11)R^2\right] + [3E - 06R] - [0.0422] \tag{9.9}$$

There is an upper threshold value of 0.19 ± 0.024 for a discharge rate of 70,000 m^3/s (+5,000 m^3/s). From the use of the equation, typical WL values from the lower threshold to the upper threshold, based on the flow-rate's data range from 1 to 21.4 cm.

9.4 Discussion

9.4.1 Freshwater Effects

The fact that the hourly streamflow data produced generally higher RMSEs than the monthly dataset indicates that the GoP's water levels are more influenced by bulk flow from the Orinoco and less by the near instantaneous flows. This may be best explained as the GoP is not directly in the river mouth, but is at some 114 km away from the main Boca (the Boca Grande). It is noted however, that there is less substantial discharge directly into the GoP. Thus, as the volumetric discharge outflows into the ocean, it loses its instantaneous characteristics due to mixing and dispersal.

Of importance to the study is the presence of other freshwater streams which may contribute to the volume of freshwater in the area, but have not been included in the modelling scenarios. The basins that provide the unaccounted for streamflows are primarily the Guarapiche Basin on the North-eastern South American continent and the Caroni River basin of Trinidad. These basins directly empty into the GoP.

The Guarapiche basin is described as the smallest, exorreica (waters reach the ocean) basin in Venezuela with an average size of about 21,000 km^2 (Machado-Allison 2012). In comparison to the Orinoco which is a significantly larger basin of about 880,000 km^2 (Sánchez-Villagra et al. 2010), the Guarapiche basin contributes a mere 2 % of freshwater by basin discharge to the ocean and the Caroni/Oropuche combined contribution from cumulative average basin sizes of about 1,616 km^2 (Environmental Management Authority 1998) – about 0.18 % compared to the Orinoco. Even at a combined contribution of near 3 % at the upper threshold of 70,000 m^3/s the rivers input an average of 2,100 m^3/s, well below the lower threshold of 10,000 m^3/s as indicated by the modelled results.

The largest external freshwater streamflow into the model domain is the Amazonian plume. The liquid volumetric discharge of the Amazon River has not been considered as the river is a considerable distance away from the GoP and while river runoff can induce large-amplitude seasonal variation of sea level in regions located near river outflows (Tsimplis and Woodworth 1994), the geographical distance of over 1,500 km, precludes the river as near. Further, the main oceanic current, the North Brazil Current (NBC) which drives the Amazonian plume northwards, retroflects before entering the model domain, this retroflection is part of the dispersal mechanism of the plume in the Atlantic. The dispersal seems more extended during the second half of the year when a large fraction of the Amazon's water flow out to deep sea as the plume flows around the NBC and is driven into the eastern Atlantic out towards Africa by the North Equatorial Counter Current (Muller-Karger et al. 1988). To account for the influence of the plume's presence as it nears the inflow boundary of the numerical model, the freshwater lenses' characteristics have however been catered to by the inclusion of the salinity changes along the boundaries.

9.4.2 Sources of Error

From the varying measures of scatter in Fig. 9.5, it is suggested that the reducing stream-flow from a stationary point (at maximum) to the decreasing limb on the hydrograph may introduce variability in phase shifts. The same is suggested for the larger variability of May as the flows increase from near minimal flows during Jan to April, although May is climatologically the windiest month of the year. These rationales may not necessarily hold for January, suggesting another driver for the degree of scatter. The largest RMSE in August also suggests the influence of another driver. It is noted that as the wind field slackens in August in the eastern Caribbean, there is a trend towards a relative maximum in sea level in the southern Caribbean due to changes in the upwelling processes. It is noted however, that these processes may not have the same effect on the GoP as there is a lack of coastal landmass between the island of Trinidad and the northeastern-most coastline of Venezuela – the Paria peninsula.

It is possible that incorporated errors may have found an avenue from not utilizing the actual discharge values from each of the water-ways. This is perhaps overcome to some extent by the utilization of the collective distribution of the discharge data to ensure that the main discharge reached the ocean. It would also be ideal to have measured data at the boundaries but the lack of availability has been addressed by using acquired, measured datasets as close as possible (spatially) to the ideal required data points.

9.4.3 Significance of Results

The results indicate that the WLs exhibit distinct seasonality mirrored by the volumetric river discharge and correlates directly to the trends on the hydrograph. Although each month's discharge/WL relationship is represented by different functions reflected in each of the scatterplots in Fig. 9.6, the lagged, bundled relation for increasing river discharge presents a definitive correlation (Fig. 9.7) indicative of the significant role of the Orinoco's discharge. The significance of the relation indicates that other individual parameters which vary across the months may not necessarily be weighted on par with the volumetric streamflow and thus may not be as influential as the stream flow.

The quasi-linear, zero sloping nature of the mean WL at the lower threshold limit indicates that the coastal WLs are largely independent of the volumetric river discharge below the threshold. The large variability on the WL therefore is more likely governed by other factors. The similar WL distribution, evident beyond the upper threshold indicates that additional discharge has little influence on the WL in the GoP. It is postulated that the reason for this is a change in the flow regime for exceedingly large volumes (approximately 70,000 m^3/s and greater). Beyond this threshold, as larger volumes of water enter the Atlantic, the momentum may take the water a greater distance across the continental shelf before the Guiana currents drives it northward, such that a smaller volume may be transported through the GoP.

The salient feature of the rising limb of the third order regression fit on the WL is the coherence of trend with the discharge rates. An increasing monthly discharge produces a corresponding increase in the WL which is signalled into the following month (but not necessarily in 1 month's time). This is not surprising as the travel time along the coast is expected to be slower than the speeds out in deeper waters. The current speeds are fastest along the edge of the continental shelf with the lower end of the range being 10 cm/s (Boisvert 1967), for a speed of 5 cm/s closer to the shore the travel time from the Boca Grande is approximately 23 days. This will of course vary with the strength of the driving currents which vary throughout the year. The effect may very well be earlier or later and this variability is reflected in the measure of scatter of the discharge/WL plot. The fairly high regression coefficients indicates that the river discharge closely drives the WL variation and although there is variation on the other parameters of salinity, wind and oceanic

currents, the range of variability is fairly small enough across the months so that the discharge effect is dominant.

9.5 Conclusion

The Orinoco River significantly modulates the water levels in the Gulf of Paria with a sigmoid-type relationship. These water levels are largely driven by bulk flow from the Orinoco with lesser dependence on the near instantaneous or daily values. The water level variation is signalled for approximately 1 month later for a given month's discharge from the river and there is a lower threshold discharge rate of $(10{,}000 \pm (2.3 \times 10^3))$ m^3/s where the water levels do not contribute more than 0.01 m of water to the variation. Above the lower threshold, the contribution may be estimated according to the derived, third order function up to an upper threshold discharge value of $(70{,}000 \pm (5 \times 10^3))$ m^3/s where the maximum amplitude of variation is estimated at 21.4 cm. This function signifies that between both lower and upper thresholds, the water levels increase for values of increasing discharge.

The study also concludes that the smaller, neighbouring rivers which have an average discharge of less than 10,000 m^3/s do not modulate the GoP's coastal water levels.

Acknowledgements The author thanks the University of the West Indies, Faculty of Engineering for the resources made available to execute the study. Acknowledgements also to the following organisations and persons for their contributions and guidance: The Global Runoff Data Centre (GRDC), The Trinidad and Tobago Meteorological Service, Dr. Julio Zyserman and the Danish Hydraulic Institute (DHI), Dr. Deborah Villarroel-Lamb, Mr. Nazeer Gopaul, Professor Arthur Mariano for his assistance with direct provision of data, Professors Jae Ryu and Lewis Williams for their guidance on watershed issue resolution.

References

Acharya A, Ryu J (2014) Simple method for streamflow disaggregation. J Hydrologic Eng 19(3):509–519

Allen PA (1997) Earth surface processes. Blackwell Science Ltd, Oxford

Antonov JI, Seidov D, Boyer TP, Locarnini RA, Mishonov AV, Garcia HE, Baranova OK, Zweng MM, Johnson DR (2010) World Ocean Atlas 2009, volume 2: salinity. NOAA Atlas NESDIS, Washington, DC, p 69

Baocan W, Jian S, Shenliang C (1992) Analysis of seasonal variation along Changjiang Estuary China. In: Woodworth PL, Pugh DT, Deronde JG, Warrick RG, Hannah J (eds) Sea level changes: determination and effects. American Geophysical Union, Washington, DC

Bjork G, Olof L, Lars R (2000) Net circulation and salinity variations in an open-ended Swedish Fijord system. Estuaries 26:367–380

Boisvert WE (1967) Major currents in the North and South Atlantic Oceans between 64°N and 60°S. U.S. Naval oceanographic technical report no. 193. United States Navy, Washington, DC

Bowles FA, Fleischer P (1985) Orinoco and Amazon River sediment input to the eastern Caribbean Basin. Mar Geol 68:53–72

Brown EB, Kraus NC (2007) Tips for developing bathymetry grids for coastal modelling systems applications, coastal and hydraulics laboratory engineering technical note ERDC/CHL CHETN-IV-69. United States Army Corps of Engineers, U (ed). U.S. Army Engineer Research and Development Center, Vicksburg

Danish Hydraulic Institute, D (2011) Mike 21 and Mike 3 flow model FM hydrodynamic and transport module scientific documentation. Danish Hydraulic Institute, Denmark

Dean RG, Walton TL (2010) Wave setup. In: Young KC (ed) Handbook of coastal and ocean engineering. World Scientific, California

Environmental Management Authority, E (1998) Trinidad and Tobago: state of the environment 1998 report. Environmental Management Authority, St. Clair

Febres-Ortega G, Herrera LE (1976) Caribbean Sea circulation and water mass transports near the Lesser Antilles. Bol Inst Oceanogr Univ Oriente 15:14

Froelich PN Jr, Atwood DK, Giese GS (1978) Influence of the Amazon River discharge on surface salinity and dissolved silicate concentration in the Caribbean Sea. Deep-Sea Res II:735–744

Gade HG (1961) On some oceanographic observations in the southeastern Caribbean Sea and the adjacent Atlantic Ocean with special reference to the influence of the Orinoco River. Bol Inst Oceanogr Univ Oriente 1:287–342

Galerkin LI (1960) On the physical basis of the forecast of the seasonal variations of sea level in the sea of Japan. Tr Inst Okeanol SSSR 37:73–91 (in Russian) in Lisitzin, E. 1974. Sea level changes. Elsevier Scientific Publishing Co, Amsterdam

Gourlay MR (1992) Wave set-up, wave run-up and beach water table: interaction between surf zone hydraulics and groundwater hydraulics. Coast Eng 17:93–144

Hsu SA (1981) Models for estimating offshore winds from onshore meteorological measurements. Bound Layer Meteorol 20:341–351

Hsu SA (1985) Correction of land-based wind data for offshore applications: a further evaluation. J Phys Oceanogr 16:390–394

Hu C, Montgomery ET, Schmitt RW, Muller-Karger FE (2004) The dispersal of the Amazon and Orinoco River water in the tropical Atlantic and Caribbean Sea: observation from space and S-PALACE floats. Deep Sea Res Part II Top Stud Oceanogr 51:1151–1171

Kolker AS, Hameed S (2007) Meteorologically driven trends in sea level rise. Geophys Res Lett 34:L23616

Lewis WM (1988) Primary production in the Orinoco River. Ecology 69:679–692

Lewis WMJ, Saunders JFI (1989) Concentration and transport of dissolved and suspended substances in the Orinoco River. Biogeochemistry 7:203–240

Lisitzin E (1974) Sea level changes, vol 8, Elsevier oceanography series. Elsevier Scientific Publishing Company, Amsterdam

Lisitzin E, Pattullo JG (1961) The principal factors influencing the seasonal oscillation of sea level. J Geophys Res 66:845–852

Loveless J, Debski D, Macleod A (1998) Sea level set-up behind detached breakwaters. In: International conference on coastal engineering, Copenhagen

Machado-Allison A (2012) Environmental impact of oil spill in Monagas unprecedented in the history of the country. Universidad Central de Venezuela, Venezuela

Mariano AJ, Brown OB (1992) Efficient objective analysis of dynamically heterogeneous and nonstationary fields via the parameter matrix. Deep-Sea Res 39:1255–1271

Mariano AJ, Ryan EH, Perkins BD, Smithers S (1995) The Mariano Global Surface Velocity Analysis 1.0 (MGSVA) U.S. Coast Guard Technical Report. CG-D-34–95

Meade RH, Emery KO (1971) Sea level as affected by river runoff, Eastern United States. Science 173:425–428

Meade RH, Nordin CF Jr, Hernandez DP, Meija A, Godoy JMP (1983) Sediment and water discharge in Rio Orinoco, Venezuela and Colombia. In: Proceedings of second international

symposium on river sedimentation. Water Resources and Electric Power Press, Beijing, pp 1134–1144
Müller-Karger FE, Mcclain CR, Richardson PL (1988) The dispersal of the Amazon water. Nature 56–59
Müller-Karger FE, Mcclain CR, Fisher TR, Esaias WE, Varela R (1989) Pigment distribution in the Caribbean Sea: observations from space. Prog Oceanogr 23:23–64
Nomitsu T, Okamoto M (1927) The causes of the annual variation of the mean sea level along the Japanese coast. Mem Coll Sci Kyoto Univ 10:125–161
Odriozola AL, Varela R, Hu C, Astor Y, Lorenzoni L, Muller-Karger FE (2007) On the absorption of light in the Orinoco River plume. Cont Shelf Res 27:1447–1464
Parker BB (ed) (1991) Tidal hydrodynamics. Wiley, New York
Pattullo J (1966) Seasonal changes in sea level. In: Hill MN (ed) The sea. Inter Science, New York
Sánchez-Villagra MR, Aguilera OA, Carlini AA (eds) (2010) Urumaco and Venezuelan paleontology: the fossil record of the Northern Neotropics. Indiana University Press, Bloomington
Schot PP, Poot A, Vonk GA, Peeters WHM (2001) A surface water model for the Orinoco River basin. A technical report. Utrecht University
Sethuraman S, Raynor GS (1980) Comparison of mean wind speeds and turbulence at a coastal site and offshore location. J Appl Meteorol 19:15–21
Stockdon HF, Holman RA, Howd PA, Sallenger AH Jr (2006) Empirical parameterization of setup, swash, and runup. Coast Eng 53:573–588
Svensson C, Jones DA (2004) Dependence between sea surge, river flow and precipitation in south and west Britain. Hydrol Earth Syst Sci 8:973–992
Trifonova E, Demireva D (2003) An investigation of sea level fluctuations in Varna and Bourgas. Proc Inst Oceanol 4:3–9
Tsimplis MN, Woodworth PL (1994) The global distribution of the seasonal sea level cycle calculated from coastal tide gauge data. J Geophys Res 99:16031–16039
TTMS TATMS (2010) MSL and wind speeds. Service TATM (ed). Ministry of Public Utilities, Government of the Republic of Trinidad and Tobago, Piarco
Van Andel TH, Postma H (1954) Recent sediments in the gulf of Paria. Reports of the Orinoco shelf expedition. Verh, der Konink-lijke Nederlandse Akad van Wetensch Afd Natuurkunde, Eerste Reeks 20:244
Warne AG, Meade RH, White WA, Guevara EH, Gibeaut J, Smyth RC, Aslan A, Tremblay T (2002) Regional controls on geomorphology, hydrology, and ecosystem integrity in the Orinoco Delta, Venezuela. Geomorphology 44:273–307